Biochemistry

pubs.acs.org/biochemistry

Communication

High-Resolution *In Situ* NMR Spectroscopy of Bacterial Envelope Proteins in Outer Membrane Vesicles

Johannes Thoma and Björn M. Burmann*

Cite This: *Biochemistry* 2020, 59, 1656−1660

Read Online

ACCESS | Metrics & More | Article Recommendations | Supporting Information

ABSTRACT: The cell envelope of Gram-negative bacteria is an elaborate cellular environment, consisting of two lipid membranes separated by the aqueous periplasm. So far, efforts to mimic this environment under laboratory conditions have been limited by the complexity of the asymmetric bacterial outer membrane. To evade this impasse, we recently established a method to modify the protein composition of bacterial outer membrane vesicles (OMVs) released from *Escherichia coli* as a platform for biophysical studies of outer membrane proteins in their native membrane environment. Here, we apply protein-enriched OMVs to characterize the structure of three envelope proteins from *E. coli* using nuclear magnetic resonance (NMR) spectroscopy and expand the methodology to soluble periplasmic proteins. We obtain high-resolution *in situ* NMR spectra of the transmembrane protein OmpA as well as the periplasmic proteins CpxP and MalE. We find that our approach facilitates structural investigations of membrane-attached protein domains and is especially suited for soluble proteins within their native periplasmic environment. Thereby, the use of OMVs in solution NMR methods allows *in situ* analysis of the structure and dynamics of proteins twice the size compared to the current *in-cell* NMR methodology. We therefore expect our work to pave the way for more complex NMR studies of bacterial envelope proteins in the native environment of OMVs in the future.

The structure, the conformation, and, consequently, the functional state of proteins are directly influenced by the surrounding environment.[1,2] Structural biology typically demands proteins be extracted from their natural cellular environment and studied under highly specialized conditions.[3,4] However, lately efforts to study proteins *in situ* using biophysical methods such as cryo-electron tomography and *in-cell* NMR spectroscopy are becoming more common.[5,6] One particularly complex cellular environment, which so far has evaded such efforts, is the cell envelope of Gram-negative bacteria, formed by two distinct membranes enclosing the periplasm, which contains a thin peptidoglycan wall. Despite more than one-third of the bacterial genome encoding envelope proteins, the envelope accounts only for 5−10% of the cellular volume.[7,8] This low volume ratio makes it complicated to study envelope proteins by established *in situ* methods (such as *in-cell* NMR spectroscopy), because envelope proteins are outnumbered by cytosolic proteins. On the contrary, the complexity of asymmetric bacterial outer membranes (the inner leaflet of which contains phospholipids, whereas the outer leaflet is formed exclusively by lipopolysaccharide) makes it impossible to mimic this unique environment to characterize envelope components in isolation by biophysical methods.

To overcome these limitations, we recently developed a new platform to study outer membrane proteins within their native membrane environment using protein-enriched outer membrane vesicles (OMVs).[9] These vesicles share the native membrane composition with the bacterial outer membrane they naturally bud from and carry periplasmic content in their lumen. OMVs can be purified from bacterial growth media in a nondestructive manner, providing an isolated cell envelope microenvironment.[10] Via overexpression of selected outer membrane proteins in *Escherichia coli* depletion strain BL21(DE3)omp8,[11] the protein composition of OMVs can be modified to contain a protein of choice at high density and purity.[9] In a pioneering study using atomic force microscopy (AFM), we demonstrated that proteins enriched in this way persisted in the membrane of OMVs in their native conformation.[9] However, because AFM can only provide low-resolution structural information, we here set out to elucidate the applicability of our OMV-based approach to obtain high-resolution structural information about envelope proteins under native conditions using NMR spectroscopy.

To this end, we prepared OMVs from BL21(DE3)omp8 enriched in the major outer membrane protein OmpA from *E. coli*, which anchors the outer membrane to the underlying peptidoglycan layer.[12] OmpA has a two-domain architecture containing an N-terminal transmembrane domain and a C-terminal soluble globular domain facilitating the interaction with the peptidoglycan. Especially the N-terminal transmembrane domain, which forms an eight-stranded β-barrel, has been extensively structurally characterized.[13−15] Due to its two-domain architecture, OmpA makes an ideal target to test our approach on the integral membrane part as well as the soluble domain. To facilitate efficient targeting of OmpA to

Received: December 30, 2019
Revised: March 27, 2020
Published: April 1, 2020

https://dx.doi.org/10.1021/acs.biochem.9b01123
Biochemistry 2020, 59, 1656−1660

OMVs, we inserted two-point mutations, D241A and R256A, which inhibit peptidoglycan binding[12,15] and result in greater enrichment of OmpA in OMVs (Figure S1A). Moreover, to obtain OmpA-enriched OMVs uniformly labeled with stable isotopes (^{2}H and ^{15}N) to perform solution-state NMR experiments, culture conditions were optimized for growth in D_2O-based M9 minimal medium (see the Experimental Section in the Supporting Information). Following isolation (Figure 1A–C), we recorded NMR spectra of OmpA-enriched OMVs. While the resulting spectra showed several resonances (Figure 1D), their ^{1}H chemical shifts were exclusively located around 8 ppm, corresponding to unstructured and flexible regions such as loops. We hypothesized that the size of OMVs and the resulting slow molecular tumbling of embedded proteins limit the spectral quality in these experiments. To optimize the size distribution of OMVs for NMR, OMVs were passed through a 50 nm liposome extruder, decreasing their diameter from 50–250 to ~50 nm (Figure 1E,F). Remeasuring the sample after extrusion resulted in substantially improved spectral quality, and multiple resonances corresponding to folded secondary structure elements could be detected (Figure 1G). Comparison to reference spectra of OmpA in solution shows that these resonances almost exclusively correspond to the C-terminal soluble domain as well as flexible loops, whereas the N-terminal transmembrane domain remains largely undetected (Figure S2). The latter can be explained not only by slower molecular tumbling rates of the transmembrane domain, compared to those of the soluble C-terminal domain, but also by the lack of back-exchange of amide protons within the membrane-embedded regions of OmpA, due to the expression in D_2O-based media. The observation of the membrane-embedded domain of OmpA or other integral membrane proteins within OMVs might therefore be more achievable by solid-state NMR approaches developed for integral membrane proteins and *in-cell* NMR.[16,17]

While this finding limits the prospect of studying transmembrane domains of outer membrane proteins in OMVs using solution NMR, it does open a unique opportunity to study soluble periplasmic proteins, given OMVs contain periplasmic proteins in a quasi-cellular context. Because the resonances that are visible in the spectrum of OmpA-enriched OMVs originated primarily from its periplasmic domain, we substituted BL21(DE3)omp8 with BL21(DE3)ΔompA,[18] to obtain OMVs containing all major porins except OmpA. The latter eliminates possible background signals originating from OmpA-CTD and results in an increased level of vesiculation compared to that of the parental BL21 strain.[18] To test the possibility of studying periplasmic proteins, we prepared OMVs luminally enriched in CpxP (Figure S1B). CpxP is a soluble protein involved in envelope stress sensing via the CpxAR two-component system with a size comparable to that of OmpA-CTD (~17 kDa). In contrast to the spectrum of OmpA, the spectrum of OMVs containing CpxP featured a set of well-resolved resonances (Figure 2) and did not require prior extrusion of the OMVs. For comparison, we recorded and assigned a reference spectrum of purified CpxP, which showed a high degree of similarity to that of CpxP-enriched OMVs (Figure S3). Comparison to spectra of OMVs prepared in the absence of protein enrichment showed that, with the exception of five strong background signals, the observed resonances could indeed be directly attributed to CpxP (Figure S4A–C). In a next step, we assessed the influence of

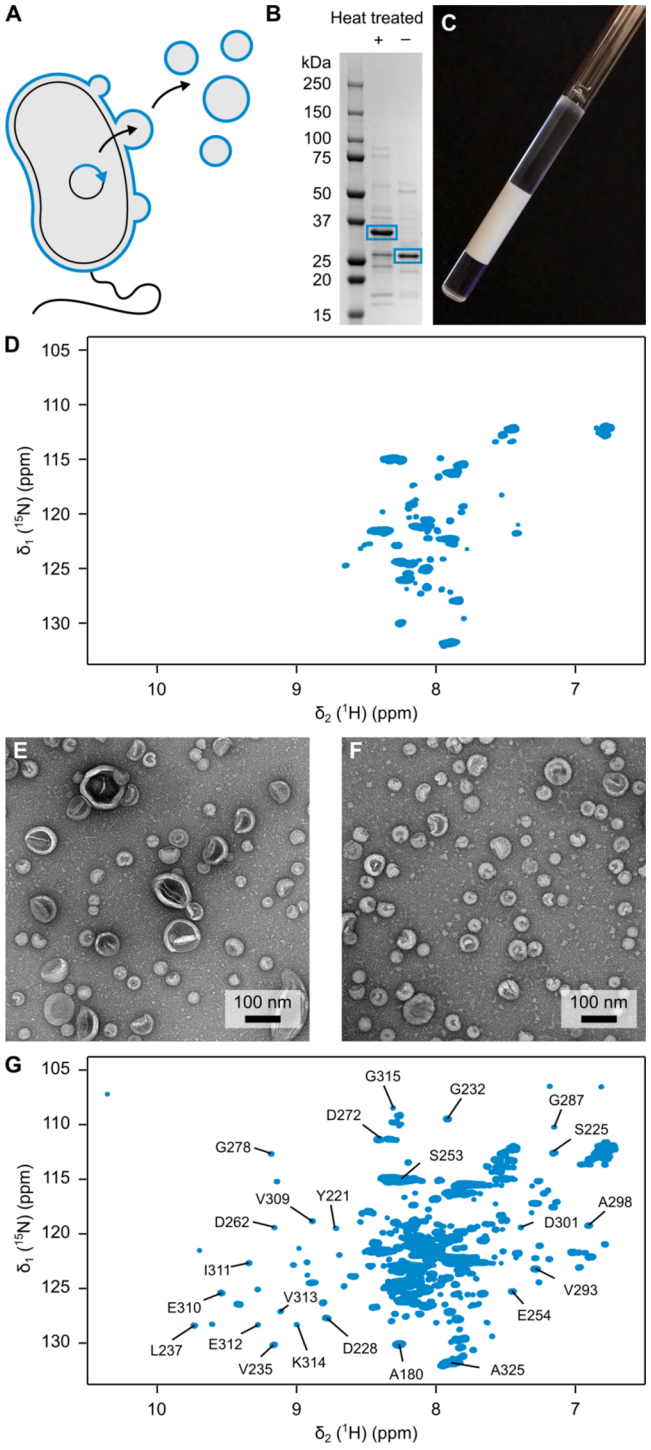

Figure 1. Preparation of OmpA-enriched OMVs. (A) Scheme for the preparation of specifically enriched OMVs. (B) Sodium dodecyl sulfate–polyacrylamide gel electrophoresis of overexpressed OmpA (blue) into OMVs. The band shift observed upon heat denaturation indicates the β-barrel fold of OmpA. (C) NMR sample of OmpA-enriched OMVs at a concentration of ~75 mg mL^{-1} in NMR buffer. (D) *In situ* two-dimensional (2D) $^{15}N-^{1}H$ TROSY HSQC spectrum of [U-^{2}H,^{15}N]OmpA measured at 37 °C in NMR buffer. (E and F) Negative stain electron microscopy of OmpA-enriched OMVs before and after extrusion, respectively, through a 50 nm cutoff membrane. Scale bars in panels E and F are 100 nm. (G) *In situ* 2D $^{15}N-^{1}H$ TROSY HSQC spectrum of [U-^{2}H,^{15}N]OmpA after extrusion, measured at 37 °C in NMR buffer. Exemplary sequence-specific resonance assignments are indicated.

https://dx.doi.org/10.1021/acs.biochem.9b01123
Biochemistry 2020, 59, 1656–1660

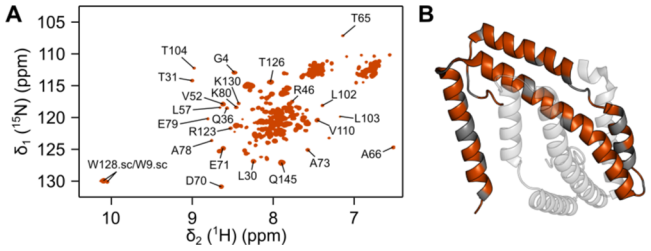

Figure 2. NMR spectroscopy of soluble proteins in OMVs. (A) 2D $^{15}N-^{1}H$ BEST-TROSY HSQC spectrum of [U-^{2}H,^{15}N]CpxP *in situ* measured at 37 °C in NMR buffer. Exemplary sequence-specific resonance assignments are indicated. (B) Cartoon representations of the crystal structure of dimeric CpxP (Protein Data Bank entry 3QZC). Observed residues are highlighted (orange) on one monomer.

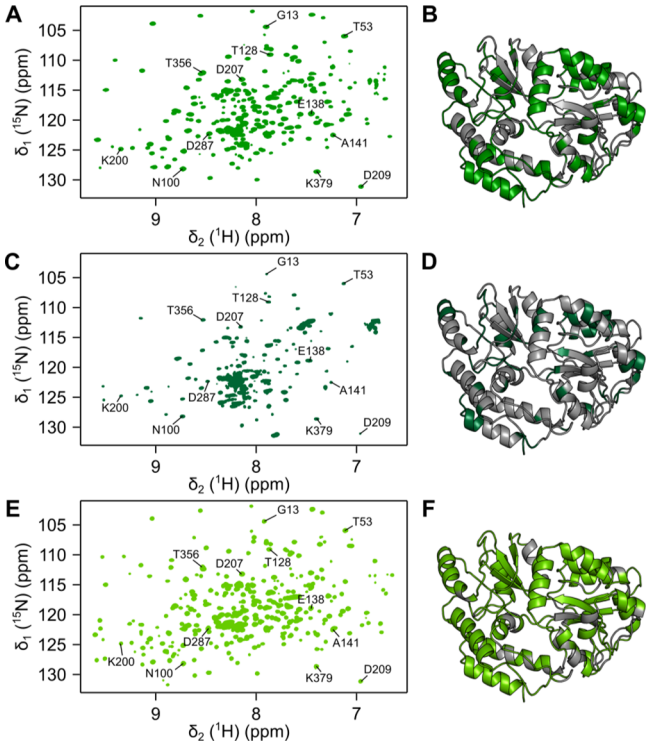

Figure 3. *In situ* and *in-cell* NMR studies of 40 kDa MBP. (A, C, and E) 2D $^{15}N-^{1}H$ BEST-TROSY HSQC spectra of [U-^{2}H,^{15}N]MBP *in situ* (green, A), *in cell* (dark green, C), and *in vitro* (light green, E). All spectra were measured at 37 °C in NMR buffer and with 120 scans. Exemplary sequence-specific resonance assignments are indicated. (B, D, and F) Cartoon representations of the crystal structure of MBP (Protein Data Bank entry 3MBP). Residues identified in *in situ* (green, B), *in-cell* (dark green, D), and *in vitro* (light green, F) NMR spectra are highlighted.

deuteration on the spectral quality; therefore, we prepared *in situ* OMV samples and *in vitro* samples of CpxP expressed in H_2O and D_2O media, respectively (Figure S4D,E). The overall spectral quality is highly similar between the proteins expressed in H_2O and D_2O showing only a few more resonances in the H_2O-derived samples indicating incomplete amide proton back-exchange. The high quality of the H_2O spectra shows that H_2O-based expression represents a suitable option for medium-sized proteins up to ∼25 kDa in OMVs. Secondary chemical shift values of the sequence-specific assigned residues of purified CpxP agree well with those of available crystal structures[19,20] (Figure 2B and Figure S3), indicating a mostly α-helical structure of purified CpxP in solution and, consequently, inside of OMVs. To assess the protein concentration inside OMVs and to test whether it resembles the concentration in the natural periplasmic environment, we used an approach adapted from *in-cell* NMR spectroscopy.[21−23] We integrated $\delta_2[^1H]$ one-dimensional cross sections from 2D $^{15}N-^{1}H$ TROSY spectra of purified CpxP at different concentrations and compared the signal intensities determined with CpxP-enriched OMVs, resulting in a total CpxP concentration of ≈86 μM in the NMR sample (Figure S5A,B). We then estimated the total vesicle volume from the turbidity of the NMR sample by first determining the vesicle radius from the slope of logarithmized optical density spectra (Figure S5C,D) followed by determining the corresponding number concentration from the optical density.[24−26] This resulted in an estimated CpxP concentration of ∼1.7 mM inside OMVs and is in agreement with values determined for periplasmic α-synuclein in previous studies.[27]

Encouraged by the high quality of the CpxP spectra, we applied the methodology to a much larger system, the 40 kDa periplasmic maltose binding protein MalE (MBP), which is frequently used as a reference standard for NMR measurements of large proteins.[28−30] We thus prepared OMVs containing high levels of MBP using BL21(DE3)ΔompA, resulting in NMR spectra of exceptional quality (Figure 3A). Compared to spectra of purified MBP, we could observe ∼50% of all resonances. The lack of completeness can be explained by insufficient back-exchange of amide protons within the solvent-inaccessible folded core of the protein, compared to *in vitro* samples that were prepared with back-exchange of amide protons by chemical denaturation. Indeed, mapping the positions of the detected resonances shows that these are mostly located on the surface of MBP (Figure 3B). Comparison to reference spectra moreover allowed us to observe that intra-OMV MBP persisted in its ligand-bound holo state.

We next set out to compare OMV NMR results to *in-cell* NMR results, which so far has been applied successfully only for small intracellular proteins of ≤15−20 kDa.[31,32] To achieve direct comparability, we performed sequential experiments from *in-cell* to *in situ* to purified and refolded MBP subsequently on the same sample preparation (Figures S1 and S6). To this end, we first expressed periplasmic MBP in BL21(DE3)ΔompA and removed a culture sample to collect an *in-cell* NMR spectrum, just before purifying OMVs from the culture supernatant (Figure 3C). We subsequently recorded a spectrum of the OMVs prepared from the same culture. Unlike the spectrum of MBP in OMVs, the *in-cell* spectrum shows only a basic resemblance to reference spectra of MBP; thus, we could identify only ∼20% of the residues of MBP (Figure 3D). For direct comparison to spectra of isolated MBP, we dissolved the OMVs by adding Triton X-100 and purified the released MBP to record a spectrum of the purified protein. The latter closely resembles that recorded for MBP in OMVs (Figure S6). We next unfolded and refolded MBP to facilitate the complete back-exchange of backbone amide protons as well as the eventual release of ligands bound to MBP. Recording a spectrum following the procedure not only increased the number of detected resonances from ∼50% to >80% but also confirmed that the conformation of MBP had changed to its apo state (Figure S6). Ultimately, we added maltose and recorded a final spectrum (Figure 3E). With the exception of

https://dx.doi.org/10.1021/acs.biochem.9b01123
Biochemistry 2020, 59, 1656−1660

the additional resonances attained through the amide proton back-exchange, the spectrum closely resembles the original *in-OMV* spectrum as well as reference spectra and shows that MBP reverted to the holo state (Figure 3F).

To relate the conditions of *in-OMV* NMR experiments to those of *in-cell* NMR experiments, we repeated the signal intensity-based concentration estimation with MBP in OMVs and *in-cell* MBP, resulting in sample concentrations of 539 and 165 μM, respectively (Figure S7). Analysis of the turbidity of the OMV sample resulted in a luminal MBP concentration of ~6.2 mM (Figure S7). In comparison, the concentration of periplasmic MBP in the *in-cell* NMR sample was estimated to be ~7.4 mM (Figure S8). While these estimated concentrations appear to be relatively high, they merely correspond to an ~7-fold increase in the level of overexpressed MBP over native periplasmic MBP levels of ~1 mM[33] and are within the limits of a suggested total periplasmic protein concentration exceeding 300 mg mL^{-1}.[27] Moreover, the high enrichment level of MBP in OMVs is reflected in the signal intensity, which matched the level of the five strong background signals otherwise observed in OMVs (Figure S7E,F). Notably, the MBP concentration was in a similar range in both samples, suggesting that the luminal environment of OMVs closely resembles the periplasmic space of the parental bacterial cells. To further elucidate the cause of the substantially increased quality of MBD spectra in OMVs compared to *in-cell*, we analyzed the line width of a subset of resonances (Figure S7G). Whereas we do not see any effects in ^{15}N line widths, we observe an average ^{1}H line width of 29 ± 7 Hz for the *in-cell* sample compared to around 19 ± 5 Hz for all other conditions, indicating a slightly more crowded environment under *in-cell* conditions, which can be explained by the slower lateral diffusion due the presence of the peptidoglycan layer,[34] or the known effect of magnetic inhomogeneity of dense cell samples.[35]

Together, our experiments clearly demonstrate the potential of protein-enriched OMVs as proxies for *in situ* studies of bacterial envelope proteins. The potential of the outlined approach thereby seems to be limited for integral outer membrane proteins, for which we could only partially resolve the soluble domain of OmpA. Unlike the case of OMVs enriched in periplasmic proteins, NMR experiments with OmpA required the OMVs to be extruded, which might entail perturbation of membrane features such as asymmetry and curvature as well as leakage of luminal proteins. In contrast, the prospect of studying soluble periplasmic proteins within their quasi-native environment is intriguing. NMR experiments with OMVs enriched in CpxP as well as MBP resulted in high-quality spectra, which allowed us to directly assess the conformation of these proteins within their cellular context. Moreover, using OMVs resulted in a vast increase in spectral quality and allowed proteins of more than twice the size to be studied compared to what has been achieved using conventional *in-cell* NMR experiments thus far. Our experiments therefore pave the way for more complex NMR studies of bacterial envelope proteins in the native environment of OMVs in the future. The usage of OMVs will be of particular advantage for proteins, which depend on specific features of the complex periplasmic environment, for example, proteins requiring the oxidative formation of disulfide bonds[36,37] or proteins affected by macromolecular crowding.[38] The ability to perform structural studies *in situ* may also improve our understanding of the mechanistic details of proteins, which occur naturally enriched in OMVs, such as virulence factors and proteins involved in quorum sensing.[39]

■ ASSOCIATED CONTENT

Supporting Information

The Supporting Information is available free of charge at https://pubs.acs.org/doi/10.1021/acs.biochem.9b01123.

Figures S1−S8 and Experimental Section (PDF)

Accession Codes

Outer membrane protein A (OmpA, UnitProtKB P0A910), periplasmic protein CpxP (UniProtKB P0AE85), and periplasmic maltose binding protein MalE (MBP, UniprotKB P0AEX9).

■ AUTHOR INFORMATION

Corresponding Author

Björn M. Burmann − *Wallenberg Centre for Molecular and Translational Medicine and Department of Chemistry and Molecular Biology, University of Gothenburg, 405 30 Göteborg, Sweden;* orcid.org/0000-0002-3135-7964; Email: bjorn.marcus.burmann@gu.se

Author

Johannes Thoma − *Wallenberg Centre for Molecular and Translational Medicine and Department of Chemistry and Molecular Biology, University of Gothenburg, 405 30 Göteborg, Sweden*

Complete contact information is available at: https://pubs.acs.org/10.1021/acs.biochem.9b01123

Funding

J.T. was supported by an EMBO Long-Term Fellowship (ALTF 413-2018). B.M.B. gratefully acknowledges funding from the Swedish Research Council (Vetenskapsrådet Starting Grant 2016-04721) and the Knut och Alice Wallenberg Foundation through a Wallenberg Academy Fellowship (2016.0163) as well as through the Wallenberg Centre for Molecular and Translational Medicine, University of Gothenburg, Sweden.

Notes

The authors declare no competing financial interest.

■ ACKNOWLEDGMENTS

The authors thank J. Croft and J. Höög (Gothenburg) for technical help with the electron microscopy experiments, A.-P. Tormänen (Oulu) for preparing the OmpA-CTD sample for sequence-specific resonance assignments, J. Perez Holmberg (Chalmers) for help with DLS measurements, and G. Grandi (Trento) for providing *E. coli* strain BL21(DE)ΔompA. The Swedish NMR Centre of the University of Gothenburg is acknowledged for spectrometer time.

■ REFERENCES

(1) Ellis, R. J. (2001) Macromolecular crowding: Obvious but underappreciated. *Trends Biochem. Sci. 26*, 597−604.

(2) Phillips, R., Ursell, T., Wiggins, P., and Sens, P. (2009) Emerging roles for lipids in shaping membrane-protein function. *Nature 459*, 379−385.

(3) Thompson, R. F., Walker, M., Siebert, C. A., Muench, S. P., and Ranson, N. A. (2016) An introduction to sample preparation and imaging by cryo-electron microscopy for structural biology. *Methods 100*, 3−15.

(4) Wiener, M. C. (2004) A pedestrian guide to membrane protein crystallization. *Methods 34*, 364−372.
(5) Briggs, J. A. G. (2013) Structural biology in situ-the potential of subtomogram averaging. *Curr. Opin. Struct. Biol. 23*, 261−267.
(6) Li, C., Zhao, J., Cheng, K., Ge, Y., Wu, Q., Ye, Y., Xu, G., Zhang, Z., Zheng, W., Zhang, X., Zhou, X., Pielak, G., and Liu, M. (2017) Magnetic resonance spectroscopy as a tool for assessing macromolecular structure and function in living cells. *Annu. Rev. Anal. Chem. 10*, 157−182.
(7) Wallin, E., and von Heijne, G. (1998) Genome-wide analysis of integral membrane proteins from eubacterial, archaean, and eukaryotic organisms. *Protein Sci. 7*, 1029−1038.
(8) Oliver, D. B. (1996) Periplasm. In *Escherichia coli and Salmonella*, pp 88−103.
(9) Thoma, J., Manioglu, S., Kalbermatter, D., Bosshart, P. D., Fotiadis, D., and Müller, D. J. (2018) Protein-enriched outer membrane vesicles as a native platform for outer membrane protein studies. *Commun. Biol. 1*, 23.
(10) Chutkan, H., MacDonald, I., Manning, A., and Kuehn, M. J. (2013) Quantitative and Qualitative Preparations of Bacterial Outer Membrane Vesicles. *Methods Mol. Biol. 966*, 259−272.
(11) Prilipov, A., Phale, P. S., Gelder, P., Rosenbusch, J. P., and Koebnik, R. (1998) Coupling site-directed mutagenesis with high-level expression: large scale production of mutant porins from *E. coli*. *FEMS Microbiol. Lett. 163*, 65−72.
(12) Park, J. S., Lee, W. C., Yeo, K. J., Ryu, K.-S., Kumarasiri, M., Hesek, D., Lee, M., Mobashery, S., Song, J. H., Kim, S. I., Lee, J. C., Cheong, C., Jeon, Y. H., and Kim, H.-Y. (2012) Mechanism of anchoring of OmpA protein to the cell wall peptidoglycan of the gram-negative bacterial outer membrane. *FASEB J. 26*, 219−228.
(13) Pautsch, A., and Schulz, G. E. (1998) Structure of the outer membrane protein A transmembrane domain. *Nat. Struct. Biol. 5*, 1013−1017.
(14) Arora, A., Abildgaard, F., Bushweller, J. H., and Tamm, L. K. (2001) Structure of outer membrane protein A transmembrane domain by NMR spectroscopy. *Nat. Struct. Biol. 8*, 334−338.
(15) Ishida, H., Garcia-Herrero, A., and Vogel, H. J. (2014) The periplasmic domain of *Escherichia coli* outer membrane protein A can undergo a localized temperature dependent structural transition. *Biochim. Biophys. Acta, Biomembr. 1838*, 3014−3024.
(16) Pinto, C., Mance, D., Julien, M., Daniels, M., Weingarth, M., and Baldus, M. (2019) Studying assembly of the BAM complex in native membranes by cellular solid-state NMR spectroscopy. *J. Struct. Biol. 206*, 1−11.
(17) Medeiros-Silva, J., Mance, D., Daniels, M., Jekhmane, S., Houben, K., Baldus, M., and Weingarth, M. (2016) ^{1}H-Detected solid-state NMR studies of water-inaccessible proteins *in vitro* and *in situ*. *Angew. Chem., Int. Ed. 55*, 13606−13610.
(18) Fantappiè, L., de Santis, M., Chiarot, E., Carboni, F., Bensi, G., Jousson, O., Margarit, I., and Grandi, G. (2014) Antibody-mediated immunity induced by engineered *Escherichia coli* OMVs carrying heterologous antigens in their lumen. *J. Extracell. Vesicles 3*, 24015.
(19) Thede, G. L., Arthur, D. C., Edwards, R. A., Buelow, D. R., Wong, J. L., Raivio, T. L., and Glover, J. N. M. (2011) Structure of the periplasmic stress response protein CpxP. *J. Bacteriol. 193*, 2149−2157.
(20) Zhou, X., Keller, R., Volkmer, R., Krauss, N., Scheerer, P., and Hunke, S. (2011) Structural basis for two-component system inhibition and pilus sensing by the auxiliary CpxP protein. *J. Biol. Chem. 286*, 9805−9814.
(21) Theillet, F. X., Binolfi, A., Bekei, B., Martorana, A., Rose, H. M., Stuiver, M., Verzini, S., Lorenz, D., van Rossum, M., Goldfarb, D., and Selenko, P. (2016) Structural disorder of monomeric α-Synuclein persists in mammalian cells. *Nature 530*, 45−50.
(22) Wider, G., and Dreier, L. (2006) Measuring protein concentrations by NMR spectroscopy. *J. Am. Chem. Soc. 128*, 2571−2576.
(23) Matečko-Burmann, I., and Burmann, B. M. (2020) Recording in-cell NMR-spectra in living mammalian cells. *Methods Mol. Biol.*, 2141.
(24) Chong, C. S., and Colbow, K. (1976) Light scattering and turbidity measurements on lipid vesicles. *Biochim. Biophys. Acta, Biomembr. 436*, 260−282.
(25) Khlebtsov, N. G., Kovler, L. A., Zagirova, S. V., Khlebtsov, B. N., and Bogatyrev, V. A. (2001) Spectroturbidimetry of Liposome Suspensions. *Colloid J. 63*, 491−498.
(26) Elsayed, M. M. A., and Cevc, G. (2011) Turbidity spectroscopy for characterization of submicroscopic drug carriers, such as nanoparticles and lipid vesicles: Size determination. *Pharm. Res. 28*, 2204−2222.
(27) Zimmerman, S. B., and Trach, S. O. (1991) Estimation of macromolecule concentrations and excluded volume effects for the cytoplasm of *Escherichia coli*. *J. Mol. Biol. 222*, 599−620.
(28) Gardner, K. H., Zhang, X., Gehring, K., and Kay, L. E. (1998) Solution NMR studies of a 42 KDa Escherichia coli maltose binding protein/β-cyclodextrin complex: Chemical shift assignments and analysis. *J. Am. Chem. Soc. 120*, 11738−11748.
(29) Tang, C., Schwieters, C. D., and Clore, G. M. (2007) Open-to-closed transition in apo maltose-binding protein observed by paramagnetic NMR. *Nature 449*, 1078−1082.
(30) Lange, O. F., Rossi, P., Sgourakis, N. G., Song, Y., Lee, H. W., Aramini, J. M., Ertekin, A., Xiao, R., Acton, T. B., Montelione, G. T., and Baker, D. (2012) Determination of solution structures of proteins up to 40 kDa using CS-Rosetta with sparse NMR data from deuterated samples. *Proc. Natl. Acad. Sci. U. S. A. 109*, 10873−10878.
(31) Banci, L., Barbieri, L., Bertini, I., Luchinat, E., Secci, E., Zhao, Y., and Aricescu, A. R. (2013) Atomic-resolution monitoring of protein maturation in live human cells by NMR. *Nat. Chem. Biol. 9*, 297−299.
(32) Tanaka, T., Ikeya, T., Kamoshida, H., Suemoto, Y., Mishima, M., Shirakawa, M., Güntert, P., and Ito, Y. (2019) High-resolution protein 3D structure determination in living eukaryotic cells. *Angew. Chem., Int. Ed. 58*, 7284−7288.
(33) Boos, W., and Shuman, H. (1998) Maltose/maltodextrin system of *Escherichia coli*: transport, metabolism, and regulation. *Microbiol. Mol. Biol. Rev. 62*, 204−2629.
(34) Brass, J. M., Higgins, C. F., Foley, M., Rugman, P. A., Birmingham, J., and Garland, P. B. (1986) Lateral diffusion of proteins in the periplasm of *Escherichia coli*. *J. Bacteriol. 165*, 787−795.
(35) Waudby, C. A., Camilloni, C., Fitzpatrick, A. W., Cabrita, L. D., Dobson, C. M., Vendruscolo, M., and Christodoulou, J. (2013) In-cell NMR characterization of the secondary structure populations of a disordered conformation of α-synuclein within *E. coli* cells. *PLoS One 8*, No. e72286.
(36) Depuydt, M., Messens, J., and Collet, J. F. (2011) How proteins form disulfide bonds. *Antioxid. Redox Signaling 15*, 49−66.
(37) Denoncin, K., and Collet, J. F. (2013) Disulfide bond formation in the bacterial periplasm: major achievements and challenges ahead. *Antioxid. Redox Signaling 19*, 63−71.
(38) Miklos, A. C., Sumpter, M., and Zhou, H. X. (2013) Competitive interactions of ligands and macromolecular crowders with maltose binding protein. *PLoS One 8*, No. e74969.
(39) Jan, A. T. (2017) Outer membrane vesicles (OMVs) of Gram-negative bacteria: A perspective update. *Front. Microbiol. 8*, 1053.

https://dx.doi.org/10.1021/acs.biochem.9b01123
Biochemistry 2020, 59, 1656−1660